Th(IV) adsorption on mesoporous molecular sieves: effects of contact time, solid content, pH, ionic strength, foreign ions and temperature

Liming Zuo · Shaoming Yu · Hai Zhou · Xue Tian · Jun Jiang

Abstract The mesoporous molecular sieves (Al-MCM-41) are synthesized with montmorillonite as silica–alumina source by hydrothermal method. The application of Al-MCM-41 for the adsorption of Th(IV) from aqueous solution is studied by batch technique. The effects of contact time, solid content, pH, ionic strength, foreign ions, and temperature are determined, and the results indicate that the adsorption of Th(IV) to Al-MCM-41 is strongly dependent on pH values but independent of ionic strength. The adsorption isotherms are simulated by D–R and Freundlich models well. The thermodynamic parameters (ΔH^0, ΔS^0, ΔG^0) are calculated from the temperature dependent adsorption isotherms at 293, 313 and 333 K, respectively, and the results suggest that the adsorption of Th(IV) on Al-MCM-41 is a spontaneous and endothermic process. Al-MCM-41 is a suitable material for the preconcentration of Th(IV) from large volumes of aqueous solutions.

Keywords Adsorption · Th(IV) · Mesoporous molecular sieves · Thermodynamic data

Introduction

The synthesis and application of mesoporous molecular sieves have received increasing attention since their first synthesized in 1992 [1]. Mesoporous molecular sieves have potential use in the catalysis, biomedicine and adsorption fields [2, 3] because of their large surface area, narrow distribution of the pore size, well-defined and adjustable pore structure. The traditional silica-containing molecular sieves are prepared using chemicals as silica sources such as tetraethoxysilane (TEOS), and the resource consumption is expensive. Recently, considerable attentions have been paid to a new process to prepare mesoporous silica from natural clays [4–6] because they are low-cost and abundant in nature. In this work, the mesoporous molecular sieves (denoted as Al-MCM-41) were prepared with montmorillonite as silica–alumina sources by the hydrothermal method [7, 8].

Thorium, which is only stable at its +IV valence in solution, is an important model element for other tetravalent actinides such as Np(IV), U(IV), and Pu(IV) [9]. The fate of Th(IV) in the environment is controlled by sorption, desorption, migration and diffusion of Th(IV) in clay minerals and oxides. A number of methodologies including evaporation, chemical precipitation, ion exchange and adsorption have been developed to remove thorium from aqueous solutions [10]. Among these methods, adsorption is one of the most widely used one in nuclear/radiation chemistry [11–13]. In recent years, the adsorption of Th(IV) on different adsorbents was studied extensively [14–19]. Tan et al. [17] studied the adsorption of Th(IV) on nano particles of anatase and found that Th(IV) adsorption increased markedly from ∼4 to 95% at pH 1.5–4.0. Chen and Wang [18] investigated the effect of pH, humic/fulvic acids, ionic strength and electrolyte type on adsorption of Th(IV) on SiO_2 and found that the adsorption of Th(IV) on SiO_2 was strongly dependent on pH and independent of ionic strength. Zhao et al. [19] also reported similar results of Th(IV) adsorption on MX-80 bentonite. Surface complexation was considered to be the main adsorption mechanism. Surface complexation was considered to be the main adsorption mechanism.

L. Zuo · S. Yu (✉) · H. Zhou · X. Tian · J. Jiang
School of Chemical Engineering, Hefei University of Technology, 230009 Hefei, Anhui, People's Republic of China
e-mail: shmyu@hfut.edu.cn

In this paper, the adsorption of Th(IV) on Al-MCM-41 as a function of contact time, solid content, pH, ionic strength, foreign ions and temperature was investigated. The basic objectives of the present work are: (1) to study the effect of contact time on the adsorption of Th(IV); (2) to study effect of solid content, pH, ionic strength, foreign ions and temperature on Th(IV) adsorption on Al-MCM-41; (3) to calculate the thermodynamic parameters of Th(IV) adsorption, such as ΔH^0, ΔS^0 and ΔG^0; (4) to describe Th(IV) adsorption isotherms with Langmuir, Freundlich and D–R models; and (5) to evaluate the adsorption mechanism of Th(IV) on Al-MCM-41.

Experimental

Material

All chemicals used in the experiments were purchased as analytical purity, and used without any further treatment. The montmorillonite sample was obtained from Huangshan country (Anhui Province, China). Sodium metasilicate ($Na_2SiO_3 \cdot 9H_2O$) was purchased from Shanghai Reagent Company. All solutions were prepared with Milli-Q water.

Preparation of mesoporous molecular sieves

The synthesis procedure of mesoporous molecular sieves was as follows: 1.0 g montmorillonite was mixed with 37 mL 0.2 mol/L NaOH solution and stirred for 30 min at room temperature. Then 1.4 g CTAB, 4.3 g sodium silicate and 9.1 g distilled water were added to this solution to obtain a molar composition of 1.0 Si:0.15 CTAB:0.1 Al:100 H_2O. The pH value of the mixture was adjusted to 10.5 by adding HCl and NaOH solution. After 1 h stirring, the mixture was loaded into a Teflon-lined stainless steel autoclave and heated at 373 K for 24 h. Then the solid phase was recovered by filtration, washed with distilled water, dried at 373 K and calcined at 873 K for 8 h. Thus derived sample was named Al-MCM-41.

Characterization

Al-MCM-41 was characterized by X-ray diffraction (XRD) and Fourier Transform Infrared (FTIR) spectroscopy. XRD pattern was obtained from a D/Max-rB X-ray diffractometer equipped with a monochromator, using Cu Kα radiation ($\gamma = 0.15406$ nm), at 2θ of 1–10°. The XRD device was operated at 40 KV and 100 mA. The FTIR measurement was carried out on a Bruker VECTOR-22 spectrometer in KBr pellet at room temperature. The effective range was from 400 cm^{-1} to 4000 cm^{-1}.

Experimental procedure

All experiments were carried out by using batch technique in polyethylene centrifuge tubes under ambient conditions. The Th(IV) stock solution was prepared by dissolution of reagent grade ThO_2 in 1 mol/L HNO_3 solution and then diluted to 100 µg/L. As Th(IV) stock solution was prepared at pH ~ 1, a certain volume of 0.1 or 1 mol/L NaOH was added in the system and then the pH values of the system were adjusted by adding negligible volumes of 0.01 mol/L $HClO_4$ or 0.01 mol/L NaOH to achieve the desired pH values. The stock solutions of Al-MCM-41 and $NaClO_4$ were pre-equilibrated for 24 h and then Th(IV) stock solution was added to achieve the desired concentration of the different components. Ionic strengths were adjusted to the desired values with 0.1 or 1.0 mol/L $NaClO_4$ solution. After the suspensions were stirred for 24 h, the solid and liquid phases were separated by centrifugation at 9000 rpm for 30 min. For adsorption isotherms, the pH was maintained to 3.4 ± 0.1.

The concentration of Th(IV) in aqueous solution was determined by spectrophotometry at 650 nm using Th(IV) ArsenazoIII complex. The amount of Th(IV) adsorbed on Al-MCM-41 was calculated from the difference between the initial concentration and the equilibrium one. The amount of Th(IV) adsorbed on Al-MCM-41 and distribution coefficient (K_d) are calculated from the following equations:

$$q = \frac{(C_0 - C_{eq}) \times V}{m} \tag{1}$$

$$K_d = (C_0 - C_{eq}) / C_{eq} \, V/m \tag{2}$$

where q is the amount of Th(IV) adsorbed on Al-MCM-41, C_0 is the initial concentration, C_{eq} is the final concentration in supernatant after centrifugation, m is the mass of Al-MCM-41 and V is the volume of the suspension.

All experimental data were the averages of duplicate or triplicate experiments. The relative errors of the data were about 5%.

Results and discussion

Characterization of AL-MCM-41

Figure 1 shows the XRD pattern of Al-MCM-41 sample. As displayed in Fig. 1, Al-MCM-41 exhibits an intense signal at about 2.2° due to [100] plane and weak signals between 2 and 4° (2θ) due to [110] and [200] planes. The three resolved peaks are the characteristic peaks of hexagonal MCM-41 mesoporous material [20]. These peaks confirm that the sample possesses the hexagonal mesophase structure as pure
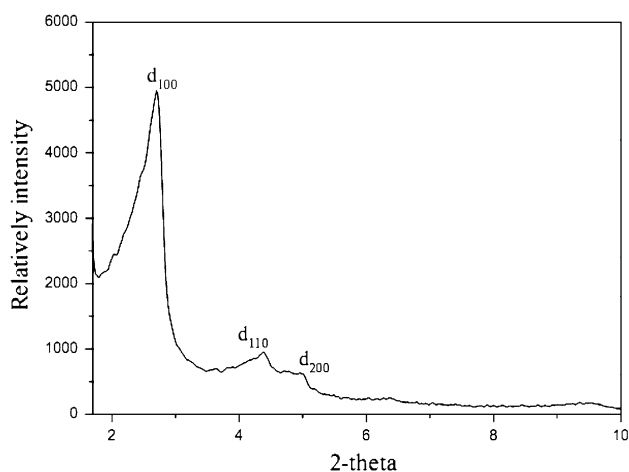
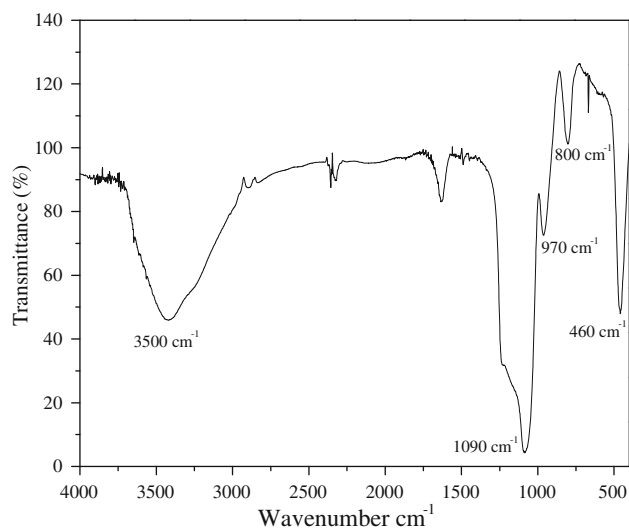**Fig. 1** XRD pattern of Al-MCM-41 sample

Fig. 2 FTIR spectrum of Al-MCM-41

silica MCM-41. The well-defined pore structure of Al-MCM-41 is due to the condensation of Si–OH groups during the calcination progress. It is noteworthy to observe that the $d(100)$ value of Al-MCM-41 is larger than that of pure silica MCM-41 and the width of $d(110)$ and $d(200)$ are broadened [20, 21]. It is proposed that this phenomenon can be due to the import of Al into the frame and thereby results in some disorder in the Al-MCM-41 sample.

Figure 2 shows the FTIR spectrum of Al-MCM-41. The broad envelope around 3500 cm^{-1} is due to O–H stretching of the framework Si–OH group and physically adsorbed water molecules [22]. The peak at 1090 cm^{-1} is attributed to the asymmetric stretching of Si–O–Si groups. The symmetric stretching modes of Si–O–Si groups are observed at ~ 800 cm^{-1} and the peak at 460 cm^{-1} is due to the bending mode of Si–O–Si, which are the characteristic adsorption peaks of SiO$_2$, indicating that the

structure of materials is not damaged after the calcinations [3, 23]. The peak at 970 cm^{-1} is assigned to the presence of defective Si–OH groups, which is the same to the characteristic adsorption peaks of silica MCM-41. Compared with FTIR spectrum of pure silica MCM-41, the characteristic peaks of Al-MCM-41 shift to lower wave number (shift from 810 to 800 cm^{-1} and 465 to 460 cm^{-1} respectively). This is because part of Si has been replaced by Al.

Effect of contact time

The effect of contact time on the adsorption of Th(IV) onto Al-MCM-41 was studied over a contact time of 0–24 h using different initial Th(IV) concentrations. Figure 3a shows that the adsorption of Th(IV) on Al-MCM-41 increases rapidly in the first contact time of 6 h and then achieves the adsorption equilibrium in 12 h. The initial rapid stage is probably due to the abundant availability of functional groups at the surface of Al-MCM-41, and with gradual utilization of these groups. The initial concentration did not have a significant effect on the contact time to achieve equilibrium. The quick adsorption of Th(IV) suggests that chemical adsorption rather than physical adsorption contributes to Th(IV) adsorption to Al-MCM-41 [24–26]. Based on these results, a contact time of 24 h was selected for the following experiments to assure the adsorption equilibrium.

In order to study the adsorption rate constant of Th(IV) to Al-MCM-41, the pseudo-second-order rate equation was used to simulate the kinetic adsorption [27]:

$$\frac{t}{q_t} = \frac{1}{2Kq_e^2} + \frac{1}{q_e}t \tag{3}$$

where q_t (mmol/g) is the amount of Th(IV) adsorbed on Al-MCM-41 at time t, and q_e (mmol/g) is the equilibrium sorption capacity. K [g/(mmol h)] is the pseudo-second-order rate constant. Constant K and q_e were calculated from the intercept and slope of the line obtained by plotting t/q_t versus t (Fig. 3b). The kinetic constants calculated by Eq. 3 are listed in Table 1. The values of K were found to decrease from 9.67 to 2.40 g/(mmol h) and the calculated q_e values increased from 0.042 to 0.116 mmol/g when the initial Th(IV) concentration increased from 0.026 to 0.086 mmol/L. All the values of regression coefficient are very close to 1, which suggests that the experimental data can be fitted very well by the pseudo-second-order model [28, 29].

Effect of solid content

Figure 4 shows the effect of Al-MCM-41 content on the removal of Th(IV). The removal percentage of Th(IV)
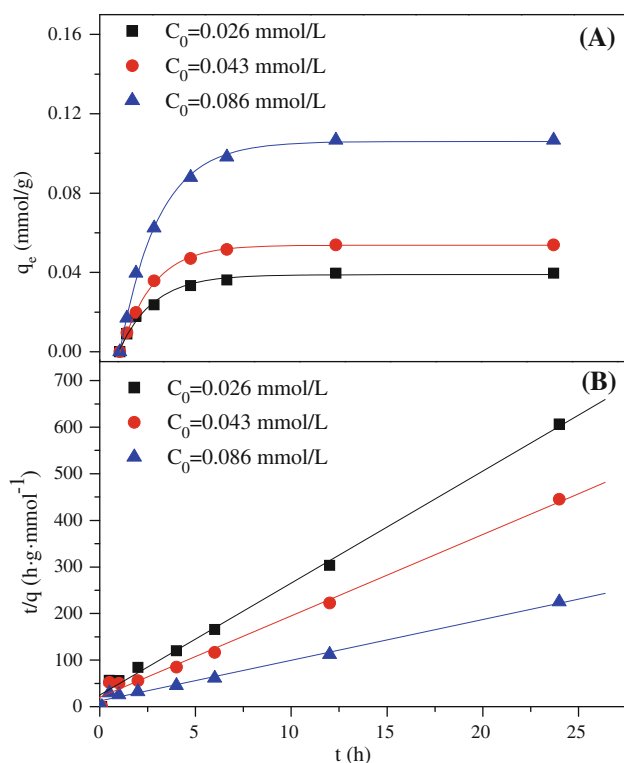
Fig. 3 Effect of Th(IV) initial concentrations and contact time on the adsorption of Th(IV) onto Al-MCM-41 (a) and the pseudo-second-order rate equation fit (b). I = 0.01 mol/L NaClO₄, m/V = 0.3 g/L, pH = 3.4 ± 0.1, T = 293 K

Table 1 Kinetic parameters for the adsorption of Th(IV) on Al-MCM-41 at different concentrations

Variable Concentration (mmol/L)	K [g/(mmol h)]	q_e (mmol/g)	R^2
0.026	9.67	0.042	0.99
0.043	5.77	0.058	0.99
0.086	2.40	0.116	0.99

increases with increasing adsorbent mass. However, the adsorption capacity decreases with increasing solid content. The decrease in concentration of Th(IV) adsorbed (q_e, mmol/g) on Al-MCM-41 with increasing adsorbent mass is due to the split in the flux or the concentration gradient between solute concentration in the solution and the solute concentration on the solid surfaces [30, 31]. Thereby, with increasing adsorbent mass, the amount of Th(IV) adsorbed onto unit weight of adsorbent gets splitted, and therefore causing a decrease in q_e value with increasing adsorbent mass content [32, 33].

Effect of pH and ionic strength

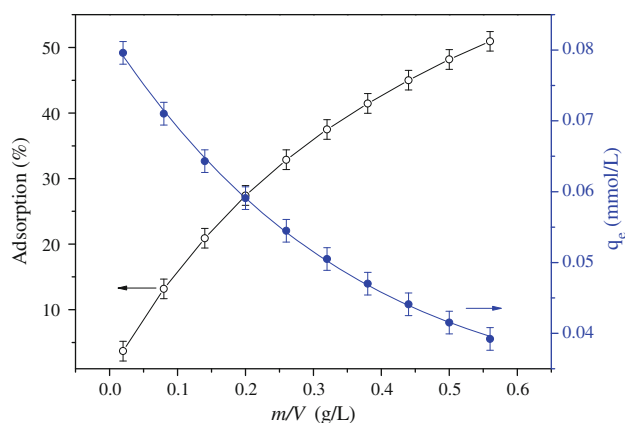Adsorption of Th(IV) on Al-MCM-41 as a function of pH in 0.1, 0.01 and 0.001 mol/L NaClO₄ solutions, respectively,

Fig. 4 Effect of solid content on the adsorption of Th(IV) to Al-MCM-41. $C_{0[Th(IV)]} = 4.31 \times 10^{-5}$ mol/L, I = 0.01 mol/L NaClO₄, pH = 3.4 ± 0.1, T = 293 K

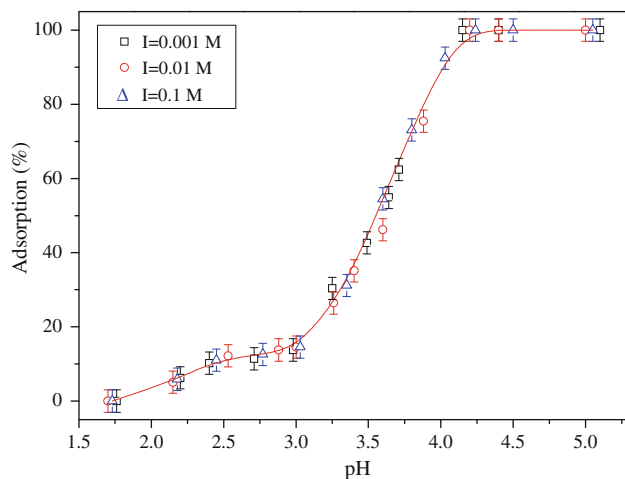
Fig. 5 Effect of pH and ionic strength on the adsorption of Th(IV) to Al-MCM-41. $C_{0[Th(IV)]} = 4.31 \times 10^{-5}$ mol/L, m/V = 0.3 g/L, T = 293 K

are shown in Fig. 5. The results show that adsorption of Th(IV) on Al-MCM-41 is obviously affected by pH values and mainly occurs at pH < 4.2. The adsorption of Th(IV) increases abruptly from ∼15 to ∼95% at pH 3.0–4.2, and then maintains high level with increasing pH at pH > 4.2. It is known that Th(IV) ions present in the forms of Th^{4+}, $Th(OH)^{3+}$, $Th(OH)_2^{2+}$, $Th(OH)_3^+$ and $Th(OH)_4$ (logk_1 = -3.86, logk_2 = -11.82, logk_3 = -24.81 and logk_4 = -41.97) at different pH values (Fig. 6) [34, 35]. As can be seen from Fig. 6, it is clear that Th(IV) starts to form precipitation at pH ∼ 4.0 if no Th(IV) is adsorbed on Al-MCM-41. However, one can see that more than 90% Th(IV) has been adsorbed to Al-MCM-41 at pH <4.0. The abrupt increase of Th(IV) adsorption at pH 3.0–4.0 is not attributed to the surface precipitation of $Th(OH)_4(S)$. The strong adsorption of Th(IV) on Al-MCM-41 is attributed to surface complexation or strong chemical adsorption [36–41]. It is
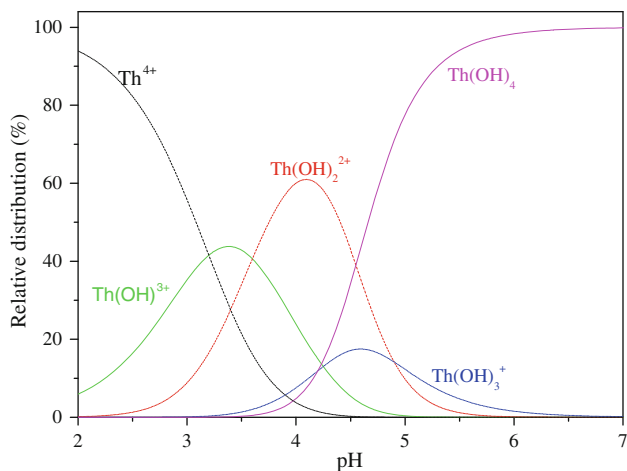
Fig. 6 Distribution of Th(IV) species as a function of pH in aqueous solutions

Fig. 7 Effect of foreign cations on Th(IV) adsorption to Al-MCM-41 as a function of pH. $T = 293$ K, m/V = 0.3 g/L, $C_{0[Th(IV)]} = 4.31 \times 10^{-5}$ mol/L

also necessary to note that the high adsorption of Th(IV) on Al-MCM-41 may also result in the precipitation of Th(IV) on Al-MCM-41. For example, at pH 3.8, nearly 80% Th(IV) is adsorbed on Al-MCM-41, surface adsorbed Th(IV) can form precipitation at lower pH because of the high local concentration of Th(IV) on Al-MCM-41 surface. The local high concentration of Th(IV) on Al-MCM-41 surface may lead to the precipitation of Th(IV) on Al-MCM-41 surfaces [42, 43].

It is well known that ClO_4^- does not form complexes with Th(IV) in solution [44]. One can see that the adsorption of Th(IV) is not influenced by $NaClO_4$ concentration, which indicates that the adsorption of Th(IV) onto Al-MCM-41 is independent of ionic strength. The ionic strength in solution may influence the double layer thickness and interface potential, and thereby can influence the binding of Th ions on Al-MCM-41[45, 46]. Outer-sphere complexes may be affected by the variations of ionic strength more easily than inner-sphere surface complexes [47]. Consequently, the adsorption of Th(IV) is assumed to form the inner-sphere surface complexes. Tan et al. [48] studied Th(IV) adsorption onto TiO_2 in KNO_3 solutions, and also found that Th(IV) adsorption was ionic strength independent. Guo et al. [49] found that the adsorption of Th(IV) on alumina decreased drastically with increasing ionic strength from 0.05 to 0.5 mol/L KNO_3 at Th(IV) concentration of 0.075–0.2 mmol/L, but increased with increasing ionic strength from 0.05 to 0.1 mol/L KNO_3 at Th(IV) concentrations <0.075 mmol/L. In general, inner-sphere surface complexation is influenced by pH values obviously, whereas ion exchange is influenced by ionic strength [50, 51]. The strong pH dependent and ionic strength independent adsorption indicate that the adsorption mechanism is mainly dominated by inner-sphere surface complexation and chemical adsorption rather than ion exchange [13, 52].
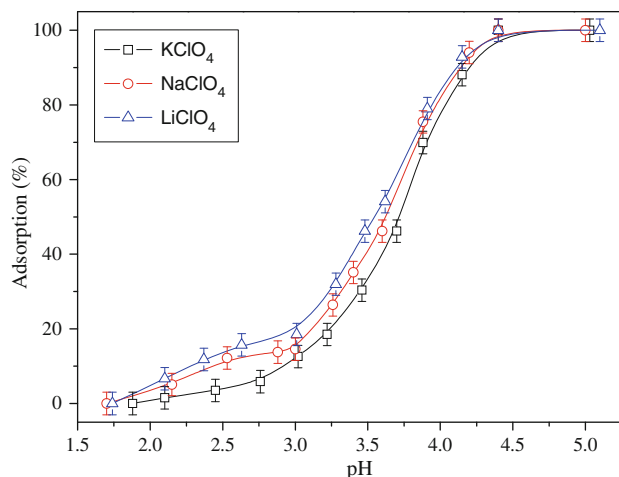
Effect of foreign cations

Figure 7 shows the effect of foreign cations on the removal of Th(IV) from aqueous solution to Al-MCM-41 in 0.01 mol/L $LiClO_4$, $NaClO_4$ and $KClO_4$, respectively, as a function of pH values. One can see that the removal of Th(IV) by Al-MCM-41 is influenced by the cations in the suspension. At pH < 4.2, the removal percentages of Th(IV) on Al-MCM-41 at the same pH values are in the following sequences: $Li^+ > Na^+ > K^+$, indicating that the cations can alter the surface properties of Al-MCM-41 and thus can influence the adsorption of Th(IV) on Al-MCM-41. Cations in solution will compete for interaction with the surface functional groups of Al-MCM-41, and Th(IV) has higher charge and has higher affinity to the surface of Al-MCM-41 than the alkali metal ions. As supported for this competition principle, the order of Th(IV) uptake under the same pH value is found to be the lowest for K^+ and the highest for Li^+, which is the order of their radius of hydration: $K^+ = 2.32$ Å, $Na^+ = 2.76$ Å and $Li^+ = 3.4$ Å [43]. The radius of Li^+ is larger than those of the other two cations and therefore the influence of Li^+ on Th(IV) adsorption is weaker than those of Na^+ and K^+. However, at pH > 4.2, no evident difference of Th(IV) adsorption to Al-MCM-41 in $LiClO_4$, $NaClO_4$ and $KClO_4$ solutions is observed, which may be attributed to surface precipitates at high pH values. The results are consistent with the adsorption of Th(IV) onto TiO_2 [48].

Effect of foreign anions

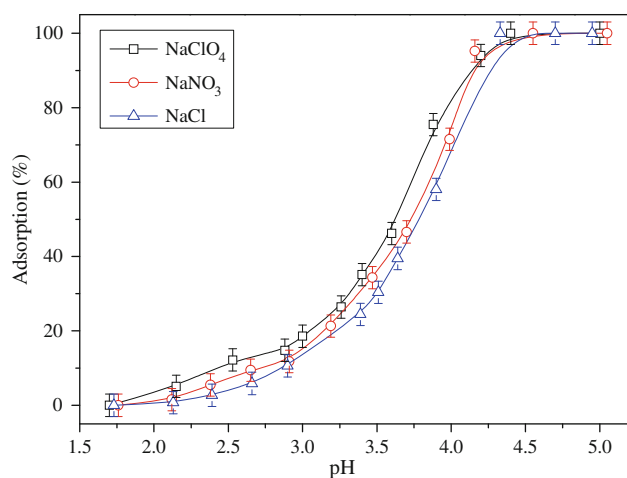Figure 8 shows the adsorption curves of Th(IV) to Al-MCM-41 as a function of pH in 0.01 mol/L $NaClO_4$,

Fig. 8 Effect of foreign anions on Th(IV) adsorption on Al-MCM-41 as a function of pH. $T = 293$ K, m/V = 0.3 g/L, $C_{0[Th(IV)]} = 4.31 \times 10^{-5}$ mol/L

NaNO$_3$ and NaCl solutions, respectively. The results demonstrate that anions affect Th(IV) adsorption to Al-MCM-41 at pH < 4.2. The adsorption percentage of Th(IV) on Al-MCM-41 is the highest in 0.01 mol/L NaClO$_4$ and the lowest in 0.01 mol/L NaCl. Cl$^-$ and NO$_3^-$ can form soluble complexes with Th(IV) (e.g. ThCl$_x^{(4-x)+}$ and Th(NO$_3$)$_x^{(4-x)+}$), while ClO$_4^-$ does not form complexes with Th(IV) in solution. Th(IV) has the highest affinity to Cl$^-$ and the lowest affinity to ClO$_4^-$ [44, 53]. Moreover, the inorganic acid radicals radium order is Cl$^-$ < NO$_3^-$ < ClO$_4^-$, the negative charged smaller radium inorganic acid radicals may form complexes with the oxygen-containing functional groups on the surfaces of Al-MCM-41 and thereby results in the decline of Th(IV) adsorption.

Adsorption isotherms and thermodynamic study data

Temperature is an important parameter that dominates the physicochemical behavior of metal ions in the environment. The adsorption isotherms of Th(IV) on Al-MCM-41 at 293, 313 and 333 K are shown in Fig. 9a. One can see that the adsorption isotherm is the highest at 333 K and is the lowest at 293 K. The results indicate that high temperature is favorable for Th(IV) adsorption onto Al-MCM-41, the results are similar to Th(IV) adsorption to zeolitic volcanic tuff [54].

The adsorption isotherms of Th(IV) were evaluated according to the Langmuir, Freundlich and D–R isotherms. The Langmuir isotherm can be represented by the following equation [53]:

$$q_e = \frac{b q_{max} C_e}{1 + b C_e} \tag{4}$$

Equation 4 can be expressed in linear form:

$$\frac{C_e}{q_e} = \frac{1}{b q_{max}} + \frac{C_e}{q_{max}} \tag{5}$$

where q_{max} and b are Langmuir constants related to adsorption capacity and adsorption energy, respectively.

The Freundlich isotherm model has the following form [55]:

$$q_e = k_F C_e^n \tag{6}$$

Equation 6 can be expressed in linear form:

$$\log q_e = \log k_F + n \log C_e \tag{7}$$

where K_F (mg^{1-n} L^n/g) represents the adsorption capacity when adsorbate equilibrium concentration equals to 1, and n represents the degree of adsorption dependence at equilibrium concentration.

The experimental data were simulated using the Dubinin–Radushkevich (D–R) equation in order to understand the adsorption type. This model is more general than the Langmuir isotherm since it does not assume a homogeneous surface or constant adsorption potential [56]:

$$q_e = q_{max} \exp(-\beta \varepsilon^2) \tag{8}$$

Equation 8 can be expressed in linear form:

$$\ln q_e = \ln q_{max} - \beta \varepsilon^2 \tag{9}$$

where q_e and q_{max} are defined above, β is the activity coefficient related to the mean sorption energy (mol^2/kJ^2), and ε is the Polanyi potential, which is equal to:

$$\varepsilon = RT \ln \left(1 + \frac{1}{C_e}\right) \tag{10}$$

where R is ideal gas constant [8.314 J/(mol K)], and T is the absolute temperature in Kelvin (K).

E (kJ mol) is defined as the free energy change that is required to transfer 1 mol of ions from solution to the solid surfaces. The relation can be expressed as follow:

$$E = \frac{1}{\sqrt{2\beta}} \tag{11}$$

The experimental data of Th(IV) adsorption are analyzed with the Langmuir, Freundlich and D–R models, and the results are shown in Fig. 9b–d. The relative constants obtained by fitting the adsorption data are listed in Table 2. It can be concluded from the correlation coefficients that Freundlich and D–R models simulate the experimental data better than Langmuir model. Al-MCM-41 has a good adsorption capacity, thus the adsorption could be better described by Freundlich model rather than by Langmuir model, since an exponentially increasing adsorption was assumed in the Freundlich model [57]. The large values of K_F indicate that Al-MCM-41 has a high adsorption affinity

Fig. 9 Adsorption isotherms (**a**), Langmuir (**b**), Freundlich (**c**) and D–R (**d**) modeling for Th(IV) adsorption on Al-MCM-41 at three different temperatures. $I = 0.01$ mol/L NaClO$_4$, pH = 3.4 ± 0.1, m/V = 0.3 g/L
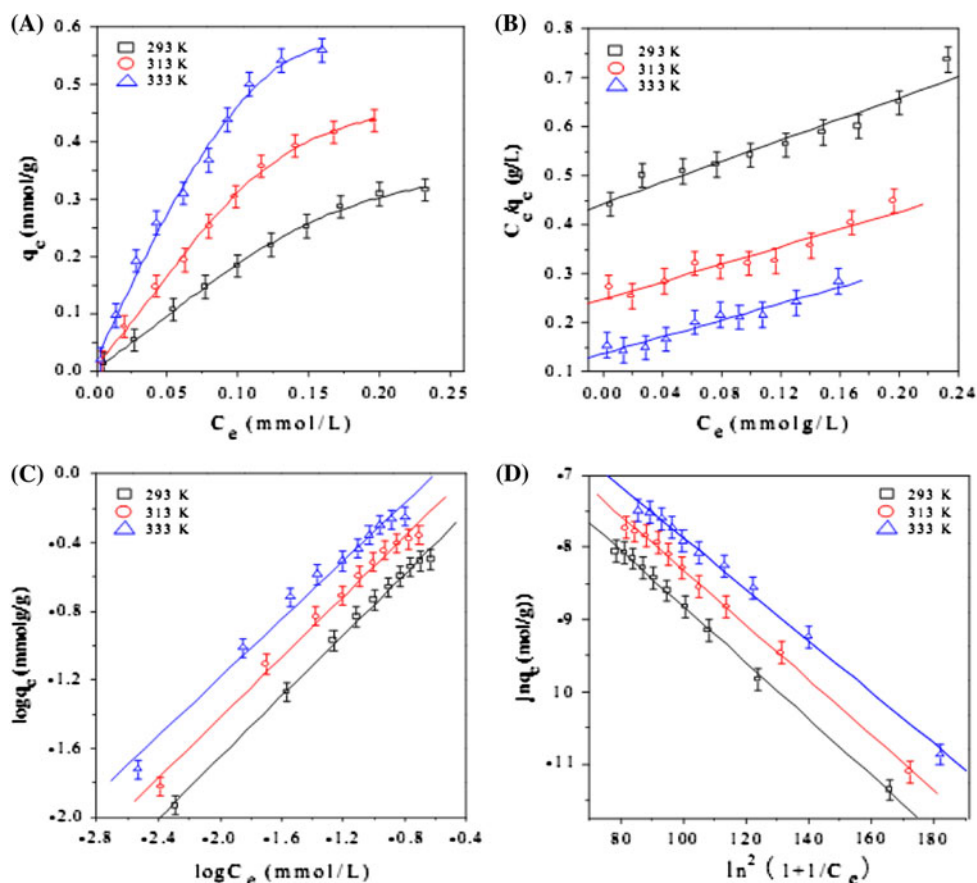
towards Th(IV). The value of n is lower than 1, which indicates that a nonlinear adsorption takes place on the heterogeneous surfaces. The Langmuir and D–R isotherms indicate that the adsorption capacity of Al-MCM-41 for Th(IV) at 293 K is in the range $\sim 1.17 \times 10^{-5}$–9.26×10^{-4} mol/g, which is consistent with the result calculated from the pseudo-second-order rate equation (5.80×10^{-5} mol/g). The magnitude of E is an important factor for estimating the adsorption mechanism. The value of E has a positive relationship with the binding ability. The E values obtained from Eq. 11 are 11.34 (293 K), 12.25 (313 K) and 13.48 KJ/mol (333 K), which are in the adsorption energy range of chemical adsorption. The results indicate that Th(IV) adsorption on Al-MCM-41 is attributed to chemical adsorption rather than physical adsorption, which is in good agreement with the effect of contact time, pH, ionic strength on Th(IV) adsorption.

The thermodynamic parameters ($\Delta G°$, $\Delta S°$, $\Delta H°$) of Th(IV) adsorption on Al-MCM-41 are calculated from the temperature dependent adsorption isotherms. The parameters are useful in defining whether the adsorption reaction is endothermic or exothermic, and the spontaneity of the adsorption process. The free energy change ($\Delta G°$) is calculated by the following equation [27]:

$$\Delta G° = -Rt \ln K°\qquad(12)$$

where R is the ideal gas constant [8.314 J/(mol K)], T (K) is the temperature in Kelvin, and $K°$ is the adsorption equilibrium constant. Values of $\ln K°$ are achieved by plotting $\ln K_d$ versus C_{eq} and extrapolating C_{eq} to zero, the value of intercept is the value of $\ln K°$ (Fig. 10).

The standard entropy change ($\Delta S°$) is calculated using the following equation:

$$\Delta S° = -(\partial \Delta G°/\partial T)_p\qquad(13)$$

The average standard enthalpy change ($\Delta H°$) is then calculated from the equation:

$$\Delta H° = \Delta G° + T\Delta S°\qquad(14)$$

The thermodynamic data calculated by Eqs. 12–14 are listed in Table 3. A positive value of the standard enthalpy change ($\Delta H°$) proves that the adsorption process of Th(IV) is endothermic. It is supported by the obvious increasing adsorption with the rise of temperature. For Th(IV) ions to get across the solution and to reach the adsorption sites, it is necessary for them firstly to be divested out of their hydration shell, and this process needs the import of energy. If the exothermicity combined with the adsorption of Th(IV) onto Al-MCM-41 is not in excess of the dehydration energy of Th(IV) ions, the entire energy balance will result in the endothermic behavior [58]. The gibbs free

Table 2 The parameters for Langmuir, Freundlich and D–R adsorption isotherms of Th(IV) on Al-MCM-41 at different temperatures

T (K)	Langmuir			Freundlich			D–R		
	q_{max} (mol/g)	b (L/mol)	R^2	k_F (mol^{1-n} L^n/g)	n	R^2	β (mol^2/kJ^2)	q_{max} (mol/g)	R^2
293	9.26×10^{-4}	2.42×10^{-3}	0.935	1.22×10^{-3}	0.842	0.991	3.89×10^{-3}	1.17×10^{-5}	0.991
313	1.12×10^{-3}	3.61×10^{-3}	0.930	1.76×10^{-3}	0.784	0.992	3.33×10^{-3}	2.98×10^{-5}	0.992
333	1.17×10^{-3}	6.27×10^{-3}	0.945	2.38×10^{-3}	0.728	0.990	2.75×10^{-3}	4.80×10^{-5}	0.994
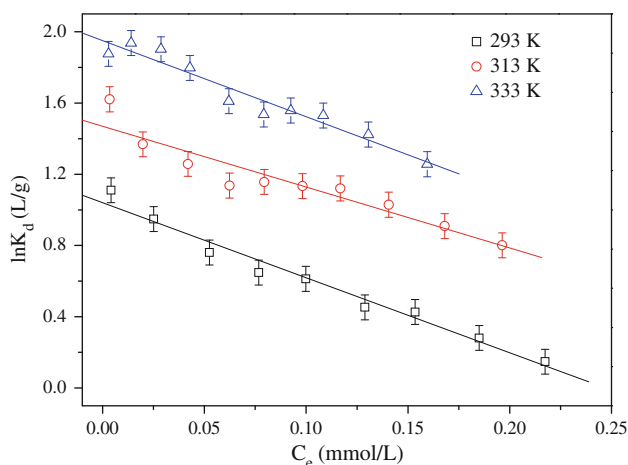
Fig. 10 Linear plots of $\ln K_d$ versus C_e for Th(IV) adsorption on Al-MCM-41 at three different temperatures. $I = 0.01$ mol/L NaClO$_4$, pH $= 3.4 \pm 0.1$, m/V $= 0.3$ g/L

Table 3 Values of thermodynamic parameters for the adsorption of Th(IV) on Al-MCM-41

T (K)	ΔG^0(J/mol)	ΔH^0 (kJ/mol)	ΔS^0 [J/(mol K)]
293	−232.30	11.63	40.45
313	−1012.06	11.55	40.45
333	−1850.33	11.63	40.45

energy change ($\Delta G°$) is negative as expected for a spontaneous process under the experimental conditions. The more negative value of $\Delta G°$ suggests more efficient adsorption of Th(IV) with the rise of temperature. The positive values of $\Delta S°$ reflect the affinity of Al-MCM-41 toward Th(IV) ions in aqueous solutions and may indicate some changes of the structure in adsorbent [59, 60].

Conclusions

Based on the results of this work, the following conclusions can be pointed out: (1) Mesoporous molecular sieves (Al-MCM-41) were synthesized with montmorillonite as silica–alumina sources; (2) The adsorption of Th(IV) on Al-MCM-41 is very fast initially and can be fitted well by a pseudo-second-order rate model; (3) The adsorption of

Th(IV) is strongly dependent on pH values and independent on ionic strength. The adsorption of Th(IV) on Al-MCM-41 is mainly dominated by surface complexation; (4) The thermodynamic data calculated from temperature dependent adsorption isotherms suggest that the adsorption reaction is spontaneous and is enhanced at higher temperature.

Al-MCM-41 has high adsorption capacity for Th(IV). Al-MCM-41 is a suitable material for removal of Th(IV) from large volumes of aqueous solutions. The adsorption of other long-lived radionuclides on Al-MCM-41 should be investigated intensively in future works. The results are important to understand the adsorption of tetravalent actinides from radionuclide contaminated solution.

References

1. Kresge CT, Leonowicz ME, Roth WJ (1992) Nature 359:710–712
2. Hartmann M (2005) Chem Mater 17:4577–4593
3. Miriam B, Debasish D, Rita F, Uwe P, Hermenegildo G (2006) Chem Mater 18:5597–5603
4. Jin SM, Xiao F, Yang HM, Qiu GZ, Yang M (2006) J Chin Ceram Soc 34:403–407
5. Zhai SR, Wei L, Yang DJ, Wu D, Sun YH (2006) Prog Chem 10:1330–1334
6. Hui KS, Chao CYH (2006) J Hazard Mater 137:1135–1148
7. Liu JF, Jing YS, Wang AP, Song B (2003) J Inorg Mater 18:867–871
8. Wu YJ, Ren XQ, Lu YD (2008) Microporous Mesoporous Mater 112:138–146
9. Guerraa DL, Vianab RR, Airoldi C (2009) J Hazard Mater 168:1504–1511
10. Hu BW, Cheng W, Zhang H, Sheng GD (2010) J Radioanal Nucl Chem 285:389–398
11. Rojo I, Seco F, Rovira M, Giménez J, Cervantes G, Mart V, Pablo J (2009) J Nucl Mater 285:474–478
12. Talip Z, Eral M, Hiçsönmez Ü (2009) J Environ Radioact 100:139–143
13. Tan XL, Fan QH, Wang XK, Grambow B (2009) Environ Sci Technol 43:3115–3121
14. Bursali EA, Merdivan M, Yurdakoc M (2010) J Radioanl Nucl Chem 283:471–476
15. Qian LJ, Zhao JN, Hu PZ, Geng YX, Wu WS (2010) J Radioanl Nucl Chem 283:653–660
16. Chen L, Gao X (2009) Appl Radiat Isot 67:1–6

17. Tan XL, Wang XL, Fang M, Chen CL (2007) Colloids Surf A 296:109–116
18. Chen CL, Wang XK (2007) Appl Radiat Isot 65:155–163
19. Zhao DL, Feng SJ, Chen CL, Chen SH, Xu D, Wang XK (2008) Appl Clay Sci 41:17–23
20. Dimos K, Stathi P, Karakassides MA, Deligiannakis Y (2009) Microporous Mesoporous Mater 126:65–71
21. Pérez-Quintanilla D, Sánchez A, delHierro I, Fajardo M, Sierra I (2007) J Colloid Interface Sci 313:551–562
22. Zhao GX, Zhang HX, Fan QH, Ren XM, Li JX, Chen YX, Wang XK (2010) J Hazard Mater 173:661–668
23. Fan QH, Shao DD, Wu WS, Wang XK (2009) Chem Eng J 150:188–195
24. Ren XM, Wang SW, Yang ST, Li JX (2010) J Radioanal Nucl Chem 283:253–259
25. Anirudhan TS, Bringle CD, Rijith SJ (2010) Environ Radioact 101:267–276
26. Hu J, Xie Z, He B, Sheng GD, Chen CL, Li JX, Chen YX, Wang XK (2010) Sci China B Chem 53:1420–1428
27. Sheng GD, Shao DD, Ren XM, Wang XQ, Li JX, Chen YX, Wang XK (2010) J Hazard Mater 178:505–516
28. Sheng GD, Hu J, Jin H, Yang ST, Ren XM, Li JX, Chen YX, Wang XK (2010) Radiochim Acta 98:291–299
29. Anirudhan TS, Suchithra PS, Rijith S (2008) Colloids Surf A 326:147–156
30. Sheng GD, Shao DD, Fan QH, Xu D, Chen YX, Wang XK (2009) Radiochim Acta 97:621–630
31. Shao DD, Fan QH, Li JX, Niu ZW, Wu WS, Chen YX, Wang XK (2009) Microporous Mesoporous Mater 123:1–9
32. Chen CL, Wang XK, Nagatsu M (2009) Environ Sci Technol 43:2362–2367
33. Fan QH, Tan XL, Li JX, Wang XK, Wu WS, Montavon G (2009) Environ Sci Technol 43:5776–5782
34. Anirudhan TS, Rijith S, Tharun AR (2010) Colloids Surf A 368:13–22
35. Choppin GR (2007) J Radioanal Nucl Chem 2763:695–703
36. Xu D, Ning QL, Zhou X, Chen CL, Tan XL, Wu AD, Wang X (2005) J Radioanal Nucl Chem 266:419–424
37. Hu J, Xu D, Chen L, Wang XK (2009) J Radioanal Nucl Chem 279:701–708
38. Chang PP, Yu SM, Chen T, Ren AP, Chen CL, Wang X (2007) J Radioanal Nucl Chem 274:153–160
39. Zhang ML, Ren AP, Shao DD, Wang X (2006) J Radioanal Nucl Chem 268:33–36
40. Yu SM, Li XG, Ren AP, Shao DD, Chen CL, Wang X (2006) J Radioanal Nucl Chem 268:387–392
41. Yu SM, Ren AP, Cheng J, Song XP, Chen CL, Wang X (2007) J Radioanal Nucl Chem 273:129–133
42. Yang ST, Li JX, Lu Y, Chen YX, Wang XK (2009) Appl Radiat Isot 67:1600–1608
43. Zhang H, Yu XJ, Chen L, Geng JQ (2010) J Radioanal Nucl Chem 286:249–258
44. Sheng GD, Hu J, Wang XK (2008) Appl Radiat Isot 66:1313–1320
45. Chen CL, Wang XK (2007) Applgeochem 22:436–445
46. Shao DD, Xu D, Wang SW, Fan QH, Wu WS, Dong YH, Wang XK (2009) Sci China B Chem 52:362–371
47. Zhao DL, Yang X, Zhang H, Chen CL, Wang XK (2010) Chem Eng J 164:49–55
48. Tan XL, Wang XK, Chen CL, Sun AH (2007) Appl Radiat Isot 65:375–381
49. Guo ZJ, Yu XM, Guo FH, Tao ZY (2005) J Colloid Interface Sci 288:14–20
50. Hu J, Chen CL, Sheng GD, Li JX, Chen YX, Wang XK (2010) Radiochim Acta 98:421–429
51. Shao DD, Jiang ZQ, Wang XK, Li JX, Meng YD (2009) J Phys Chem B 113:860–864
52. Chen CL, Xu D, Tan XL, Wang X (2007) J Radioanal Nucl Chem 273:227–233
53. Yang ST, Li JX, Shao DD, Hu J, Wang XK (2009) J Hazard Mater 166:109–116
54. Humelnicu D, Drochioiu G, Sturza MI, Cecal A, Popa K (2006) J Radioanl Nucl Chem 270:637–640
55. Tan XL, Fang M, Li JX, Lu Y, Wang XK (2009) J Hazard Mater 168:458–465
56. Wang SW, Dong YH, He ML, Chen L, Yu XJ (2009) Appl Clay Sci 43:164–171
57. Shahwan T, Erten HN (2002) J Radioanal Nucl Chem 253:115–120
58. Tan XL, Chang PP, Fan QH, Zhou X, Yu SM, Wu WS, Wang XK (2008) Colloid Surf A 328:8–14
59. Fan QH, Shao DD, Hu J, Wu WS, Wang XK (2008) Surf Sci 602:778–785
60. Tan XL, Chen CL, Yu SM, Wang XK (2008) Appl Geochem 23:2767–2777